

The oscillation effects on thermalization of the neutrinos in the universe with low reheating temperature

Kazuhide Ichikawa, Masahiro Kawasaki and Fuminobu Takahashi

*Institute for Cosmic Ray Research,
University of Tokyo, Kashiwa 277 8582, Japan*

(Dated: December 2, 2024)

Abstract

We study how the oscillations of the neutrinos affect their thermalization process during the reheating period with temperature $O(1)$ MeV in the early universe. We follow the evolution of the neutrino density matrices and investigate how the predictions of big bang nucleosynthesis vary with the reheating temperature. For the reheating temperature of several MeV, we find that including the oscillations makes different predictions, especially for ^4He abundance. Also, the effects on the lower bound of the reheating temperature from cosmological observations are discussed.

I. INTRODUCTION

The standard big bang model assumes that the universe was once dominated by thermal radiation composed of photons, electrons, neutrinos, and their anti-particles. It is one of the main issues in theories beyond the standard cosmology where these particles came from, or equivalently, what reheated the universe. The reheating temperature, at which the universe becomes radiation-dominated, is therefore a very important parameter that discriminates among many scenarios on the thermal history of the universe. In the following we define the reheating temperature as that of the latest reheating process, if the universe experienced several reheating stages.

Recent observations of the cosmic microwave background radiation (CMB) [1] has strongly suggested that the universe underwent inflation at an early stage. After inflation ended, the universe was dominated by the oscillation energy of the inflaton until it decayed and reheated the universe. The upper limit on the reheating temperature was obtained [2] by constraining the relic abundance of the gravitinos, the superpartner of the graviton, which are inevitably present in the supersymmetric (SUSY) framework. Here we are interested in the relatively low reheating temperature, especially in the MeV range, and would like to put a lower limit on the reheating temperature.

The MeV-scale reheating is actually ubiquitous in theories beyond the standard cosmology. In the framework of the SUSY and superstring theories, there are many particles with very long lifetime, e.g., the moduli and the gravitinos mentioned above, since their interaction is so weak, typically suppressed by the Planck scale. These long-lived massive particles might have dominated over the radiation from the inflaton decay. If the masses of these particles are heavy enough, they decay and reheat the universe again just before the big bang nucleosynthesis (BBN) starts. Otherwise they often cause cosmological disaster known as “cosmological moduli problem” [3, 4, 5] and “gravitino problem” [2, 6, 7, 8]. The simplest solution of these problems is to dilute the unwanted relics by producing large entropy at a later time [9, 10]. In either case, the reheating temperature is very low and typically around MeV.

Another example that prefers the low reheating temperature is the curvaton scenario [11] in which the curvaton field dominates the universe and its isocurvature fluctuation is transformed into an adiabatic one. Furthermore, in the Affleck-Dine mechanism [12] responsible

for the origin of the baryon asymmetry, it is known that non-topological solitons such as Q -balls [13] are generally created. Since the decay process of the Q -balls is geometrically suppressed, they might dominate the universe, and such possibility has been extensively studied in many different scenarios [14, 15, 16, 17].

What if the reheating temperature is several MeV? In contrast to electrons that are always (at least until the temperature drops below a few eV) in thermal contact with photons via electromagnetic forces, neutrinos interact with electrons and themselves only through the weak interaction. The decoupling temperature of the neutrinos should be around 3 MeV for the electron neutrinos and 5 MeV for the muon and tau neutrinos, respectively [18, 19, 20]. The difference comes from the fact that the electron neutrinos have additional charged current interaction with electrons. Therefore the neutrinos might not be fully thermalized if the reheating temperature is in the MeV range. If this is the case, the expansion rate of the universe becomes smaller, which affects the light element abundances and the CMB angular power spectrum [21, 22, 23]. In particular it has been widely believed or taken for granted that the predicted abundance of ^4He decreases as the reheating temperature drops below a few MeV. This is because the smaller expansion rate delays the decoupling of the neutron-proton transformation, decreasing the neutron-to-proton ratio at the beginning of the BBN. Since almost all the neutrons are absorbed in the ^4He nuclei, such a naive reasoning can explain the dependence of the ^4He abundance on the reheating temperature. In this paper, however, we will see that this widespread picture is drastically changed if we take account of the neutrino oscillations.

Recent neutrino oscillation experiments [24, 25] have determined the mass differences and mixing angles with high precision and established that mixing angles are large. The crucial point is that a flavor eigenstate transforms itself into another one. Therefore we must take special care to calculate neutrino distribution functions and the resultant effective number of neutrinos. As pointed out in Ref. [26], it is useful to follow the evolution of the neutrino density matrices when flavor mixings are present. Here we will solve momentum dependent Boltzmann equations for the neutrino density matrices. As far as we know this is the first attempt to numerically solve the neutrino collision terms including the oscillations in momentum space. We will see that the predicted abundance of ^4He is drastically changed, while the effective number of neutrinos does not change much. To put it simply, the reason for this is that the number density of the electron neutrinos is decreased due to flavor

mixings, which makes the freeze-out temperature of the neutrons higher; this effect cancels and even exceeds that of the decrease in the expansion rate. Thus MeV-scale reheating scenario is one of the examples in which the neutrino oscillations play an essential role.

The outline of this paper is the following. In the next section we formulate neutrino thermalization including flavor mixings, and derive an evolution equation of the neutrino density matrix. In the section III we will show how the predicted abundances of the light elements are modified when the reheating temperature is in the MeV range, and discuss their implications. Finally we present our conclusion in the section IV.

II. NEUTRINO THERMALIZATION

In this section, we illustrate the formulation needed to follow the neutrino thermalization process. The case without the neutrino oscillations is studied by Refs. [21, 22, 23]. Although subjects of study are different from this paper, issues of the neutrino spectrum evolution using momentum dependent Boltzmann equations in the early universe are treated in Refs. [18, 19, 20, 27, 28, 29, 30]. Our formulation almost goes in parallel with the no-mixing case and we use some of the useful techniques discussed in those papers. However, there is a very important exception that neutrino distribution functions have to be extended to neutrino density matrices [26] in order to include oscillations.

First of all, let us explain our assumptions on the reheating process and the neutrino oscillations. We refer to the massive particles which reheat the universe, or inflaton, as ϕ ¹. We assume ϕ only decays into photons (they in turn produce electrons and positrons and they all thermalize very quickly by the electromagnetic interaction). In other words, the branching ratios to neutrinos or hadrons are assumed to be negligible and neutrinos are produced exclusively via the electron-positron annihilation. Then ϕ is characterized simply by its decay rate Γ . We parametrize it by the reheating temperature T_R which is defined as

$$\Gamma = 3H(T_R), \quad (1)$$

where H is the expansion rate of the universe. Here, we use the Friedmann equation $H^2 = \rho_{\text{tot}}/3M_{\text{Pl}}^2$ where the reduced Planck mass $M_{\text{Pl}} = 2.435 \times 10^{18}$ GeV. The total energy density ρ_{tot} which consists of the radiation including photons, electrons, and three

¹ Hereafter we call ϕ as inflaton even if it is not responsible for inflation.

species of neutrinos, is expressed as $\rho_{\text{tot}} = (g_*\pi^2/30)T_R^4$ where the relativistic degree of freedom $g_* = 43/4$. This leads to

$$\Gamma = 3.26 \frac{T_R^2}{M_{\text{Pl}}} = 2.03 \left(\frac{T_R}{\text{MeV}} \right)^2 \text{sec}^{-1}. \quad (2)$$

It should be noted that, even if the neutrinos are not fully thermalized, we stick to Eq. (2) as the definition of T_R to avoid unnecessary confusion.

We consider three active flavors of neutrinos: ν_e , ν_μ and ν_τ . When the oscillations are neglected as in Refs. [21, 22, 23], there are only two sets of variables required to describe the neutrino evolution. They are the distribution functions for ν_e and ν_μ which have to be distinguished since they interact differently with electrons; ν_e interacts via both neutral and charged currents while ν_μ and ν_τ has only the former interaction. Since ν_μ and ν_τ interact with electrons identically, we do not need to solve for the distribution function of ν_τ . It is same as ν_μ 's. On the contrary, when we include the oscillations among them, ν_μ and ν_τ also have to be distinguished because their oscillations between ν_e are known to be different. Namely, we need to consider general three-flavor oscillations which require 9 real variables to fully describe our issue. However, if θ_{13} is zero, a simplification to two-flavor oscillations is possible by using non-mixing mass eigenstates ν'_μ and ν'_τ instead of ν_μ and ν_τ ². Then ν'_μ and ν_e are described by two-flavor oscillations and ν'_τ decouples from the oscillations. ν'_τ just interacts with e^\pm via neutral current and should behave as ν_τ (or ν_μ) in the no-mixing case.

Under those assumptions, the variables necessary for simulating thermalization of oscillating neutrinos are: the inflaton energy density ρ_ϕ , the photon temperature T , the ν_e - ν'_μ two-flavor neutrino density matrix ρ_p and the ν'_τ distribution function $f_{\nu'_\tau}(p)$. ρ_p and $f_{\nu'_\tau}$ are functions of neutrino momentum p . ρ_p is defined by expectation value of the product of the creation and annihilation operators [26]:

$$\left\langle a_j^\dagger(\mathbf{p}) a_i(\mathbf{q}) \right\rangle \equiv (2\pi)^3 \delta^{(3)}(\mathbf{p} - \mathbf{q}) [\rho_p]_{ij}, \quad \{i, j\} = \{e, \mu\}, \quad (3)$$

where $a_i(\mathbf{p})$ is the annihilation operator for negative-helicity neutrino of flavor i with momentum \mathbf{p} . Readers should bear in mind that the density matrix ρ_p is just an extension

² Similar simplification is shown to be useful to analyze the evolution of neutrino-antineutrino asymmetries by Refs. [31, 32].

of the occupation number to the mixed neutrinos, and should not confuse with the energy density, to which we refer as ρ_ν , ρ_ϕ , etc. Each diagonal component of ρ_p is the neutrino distribution of the corresponding flavor, while the off-diagonal ones represent more subtle information on the correlation. For anti-neutrinos we can similarly define the density matrix $\bar{\rho}_p$:

$$\left\langle b_i^\dagger(\mathbf{p}) b_j(\mathbf{q}) \right\rangle \equiv (2\pi)^3 \delta^{(3)}(\mathbf{p} - \mathbf{q}) [\bar{\rho}_p]_{ij}, \quad \{i, j\} = \{e, \mu\}, \quad (4)$$

where $b_i(\mathbf{p})$ is the annihilation operator for positive-helicity neutrino of flavor i with momentum \mathbf{p} . However, unless the lepton asymmetry is very large, we do not have to distinguish neutrinos from anti-neutrinos. In this case they are related to each other as $\bar{\rho}_p = \rho_p^T$. We next derive the differential equations which govern their evolutions.

We use scale factor a as a time variable and later we use $y \equiv pa$ instead of a momentum [19]. Then the time evolution equation for the neutrino density matrix ρ_p is [26]

$$Ha \frac{d\rho_p}{da} = -i[\Omega(p), \rho_p] + I_{\text{coll}}(p). \quad (5)$$

The matrix $\Omega(p)$ represents both the vacuum oscillations and the refractive term. Neglecting lepton asymmetry, which is usually as small as the baryon asymmetry, it is written as

$$\Omega(p) \equiv \Omega_V(p) - \frac{8\sqrt{2}G_F p}{3m_W^2} E, \quad (6)$$

where the Fermi coupling constant $G_F = 1.16637 \times 10^{-11} \text{ MeV}^{-2}$, W boson mass $m_W = 80 \text{ GeV}$. In the ultrarelativistic limit, $\Omega_V(p)$ is given by

$$\Omega_V(p) = \frac{1}{2p} U M^2 U^T, \quad (7)$$

where M^2 , the neutrino mass matrix, and U , the matrix which relates mass eigenstates and flavor eigenstates, are

$$M^2 \equiv \begin{pmatrix} m_1^2 & 0 \\ 0 & m_2^2 \end{pmatrix}, \quad U \equiv \begin{pmatrix} \cos \theta_{12} & \sin \theta_{12} \\ -\sin \theta_{12} & \cos \theta_{12} \end{pmatrix}. \quad (8)$$

We use the solar neutrino oscillation experiment values for neutrino parameters: $m_2^2 - m_1^2 = 7.3 \times 10^{-5} \text{ eV}^2$ and $\sin^2 \theta_{12} = 0.315$ [33]³. The second term in Eq. (6) comes from the

³ The most recent result [25] gives a slightly higher value of the mass squared difference: $m_2^2 - m_1^2 = 7.9_{-0.5}^{+0.6} \times 10^{-5} \text{ eV}^2$. However, we have confirmed that our results do not change for $m_2^2 - m_1^2$ in the error range.

non-local effect of the W -exchange interactions, and E is the energy density matrix of the charged leptons:

$$E = \begin{pmatrix} \rho_e + \rho_{\bar{e}} & 0 \\ 0 & 0 \end{pmatrix} = \begin{pmatrix} (7/60)\pi^2 T^4 & 0 \\ 0 & 0 \end{pmatrix}, \quad (9)$$

where $\rho_{e(\bar{e})}$ is the energy density of electrons (positrons) and we have assumed that neither muons nor taus exist in the plasma.

For the collision term I_{coll} , we consider the processes $\nu + e^\pm \leftrightarrow \nu + e^\pm$ and $\nu + \bar{\nu} \leftrightarrow e^- + e^+$. In calculating the collision term, we take electrons to be massless and neglect processes of scattering among neutrinos as Refs. [21, 22, 23]. The contributions from each process are

$$\begin{aligned} I_{\nu e \nu e}(p_1) &= \frac{1}{2E_1} \int \frac{d\mathbf{p}_2}{2E_2} \frac{d\mathbf{p}_3}{2E_3} \frac{d\mathbf{p}_4}{2E_4} (2\pi)^4 \delta^{(4)}(p_1 + p_2 - p_3 - p_4) \\ &\times 2^5 G_F^2 \left[4(p_1 \cdot p_2)(p_3 \cdot p_4) F_{LL}(\nu^{(1)}, e^{(2)}, \nu^{(3)}, e^{(4)}) \right. \\ &\quad \left. + 4(p_1 \cdot p_4)(p_2 \cdot p_3) F_{RR}(\nu^{(1)}, e^{(2)}, \nu^{(3)}, e^{(4)}) \right], \end{aligned} \quad (10)$$

$$\begin{aligned} I_{\nu \bar{e} \nu \bar{e}}(p_1) &= \frac{1}{2E_1} \int \frac{d\mathbf{p}_2}{2E_2} \frac{d\mathbf{p}_3}{2E_3} \frac{d\mathbf{p}_4}{2E_4} (2\pi)^4 \delta^{(4)}(p_1 + p_2 - p_3 - p_4) \\ &\times 2^5 G_F^2 \left[4(p_1 \cdot p_4)(p_2 \cdot p_3) F_{LL}(\nu^{(1)}, \bar{e}^{(2)}, \nu^{(3)}, \bar{e}^{(4)}) \right. \\ &\quad \left. + 4(p_1 \cdot p_2)(p_3 \cdot p_4) F_{RR}(\nu^{(1)}, \bar{e}^{(2)}, \nu^{(3)}, \bar{e}^{(4)}) \right], \end{aligned} \quad (11)$$

$$\begin{aligned} I_{\nu \bar{\nu} e \bar{e}}(p_1) &= \frac{1}{2E_1} \int \frac{d\mathbf{p}_2}{2E_2} \frac{d\mathbf{p}_3}{2E_3} \frac{d\mathbf{p}_4}{2E_4} (2\pi)^4 \delta^{(4)}(p_1 + p_2 - p_3 - p_4) \\ &\times 2^5 G_F^2 \left[4(p_1 \cdot p_4)(p_2 \cdot p_3) F_{LL}(\nu^{(1)}, \bar{\nu}^{(2)}, e^{(3)}, \bar{e}^{(4)}) \right. \\ &\quad \left. + 4(p_1 \cdot p_3)(p_2 \cdot p_4) F_{RR}(\nu^{(1)}, \bar{\nu}^{(2)}, e^{(3)}, \bar{e}^{(4)}) \right], \end{aligned} \quad (12)$$

where we define $d\mathbf{p} \equiv d^3\mathbf{p}/(2\pi)^3$, $E_i \equiv p_i^0$, and

$$\begin{aligned} F_{ab}(\nu^{(1)}, e^{(2)}, \nu^{(3)}, e^{(4)}) &\equiv \frac{1}{2} [(1 - \rho_{p_1}) G_a \rho_{p_3} G_b (1 - f_e(p_2)) f_e(p_4) + \text{h.c.} \\ &\quad - \rho_{p_1} G_a (1 - \rho_{p_3}) G_b f_e(p_2) (1 - f_e(p_4)) + \text{h.c.}], \end{aligned} \quad (13)$$

$$\begin{aligned} F_{ab}(\nu^{(1)}, \bar{e}^{(2)}, \nu^{(3)}, \bar{e}^{(4)}) &\equiv \frac{1}{2} [(1 - \rho_{p_1}) G_a \rho_{p_3} G_b (1 - f_{\bar{e}}(p_2)) f_{\bar{e}}(p_4) + \text{h.c.} \\ &\quad - \rho_{p_1} G_a (1 - \rho_{p_3}) G_b f_{\bar{e}}(p_2) (1 - f_{\bar{e}}(p_4)) + \text{h.c.}], \end{aligned} \quad (14)$$

$$\begin{aligned} F_{ab}(\nu^{(1)}, \bar{\nu}^{(2)}, e^{(3)}, \bar{e}^{(4)}) &\equiv \frac{1}{2} [(1 - \rho_{p_1}) G_a (1 - \bar{\rho}_{p_2}) G_b f_e(p_3) f_{\bar{e}}(p_4) + \text{h.c.} \\ &\quad - \rho_{p_1} G_a \bar{\rho}_{p_2} G_b (1 - f_e(p_3)) (1 - f_{\bar{e}}(p_4)) + \text{h.c.}], \end{aligned} \quad (15)$$

with $G_L = \text{diag}(g_L, \tilde{g}_L)$ and $G_R = \text{diag}(g_R, g_R)$. Here, $\tilde{g}_L = g_L - 1 = \sin^2 \theta_W - \frac{1}{2}$ and $g_R = \sin^2 \theta_W$ where $\sin^2 \theta_W = 0.23120$ is the weak-mixing angle. $f_e(f_{\bar{e}})$ is the distribution

function of electrons (positrons). Hereafter we take $\bar{\rho}_p = \rho_p^T$ and $f_{\bar{e}} = f_e$. Note that these collision terms coincide with those found in Ref. [19] if oscillations are absent (i.e., if off-diagonal components in the density matrices are zero).

We further approximate that electrons obey the Boltzmann distribution and their Pauli blocking factors are neglected. Namely, in F 's, we replace as $f_e(p) \rightarrow \exp(-p/T)$ and $1 - f_e(p) \rightarrow 1$. Then the collision terms above are reduced to one-dimensional momentum integration by the technique in Ref. [22] and the reduced expressions become equal to the ones in the reference ⁴ in the limit of the zero mixing angle.

In practice, since ρ_p is 2×2 Hermitian matrix, it is convenient to expand it using Pauli matrices. Namely,

$$\rho_p = \sum_{i=0}^3 P_i(p) \frac{\sigma_i}{2}, \quad (16)$$

where

$$\sigma_0 \equiv \begin{pmatrix} 1 & 0 \\ 0 & 1 \end{pmatrix}, \quad \sigma_1 \equiv \begin{pmatrix} 0 & 1 \\ 1 & 0 \end{pmatrix}, \quad \sigma_2 \equiv \begin{pmatrix} 0 & -i \\ i & 0 \end{pmatrix}, \quad \sigma_3 \equiv \begin{pmatrix} 1 & 0 \\ 0 & -1 \end{pmatrix}. \quad (17)$$

On the right hand side of Eq. (5), $i[\Omega, \rho_p]$ and I_{coll} , are expanded similarly. We solve for the evolution of $P_0 \sim P_3$ and the distributions of ν_e and ν'_μ are in turn derived by $f_{\nu_e} = (P_0 + P_3)/2$ and $f_{\nu'_\mu} = (P_0 - P_3)/2$. The evolution equations are formally written as

$$Ha \frac{dP_i(y)}{da} = -i\Omega_i(y) + I_i(y), \quad (18)$$

where i runs from 0 to 3, $\Omega_i \equiv \text{Tr}([\Omega, \rho_p] \sigma_i)$ and $I_i \equiv \text{Tr}(I_{\text{coll}} \sigma_i)$, and we have changed the variable p to y .

We need to solve for the evolution of ν'_τ , too. To this end, it is most simple to obtain the time evolution of $f_{\nu'_\tau}$ from the ν'_μ -component of Eq. (5) with no mixing (which is given by omitting the first term on the right hand side) because the interactions of ν'_τ with e^\pm are same as those of ν'_μ .

⁴ The right hand side of Eq. (A16) in Ref. [22] has to be multiplied by 2 to be a correct equation. Due to this error, the right hand side of Eq. (3) in Ref. [21] has to be multiplied by 2. The right hand side of Eq. (12) in Ref. [22] has to be multiplied by 8 since it had already contained a typo of factor 4. In this occasion, we correct a typo in the right hand side of Eq. (8) in Ref. [22]: it has to be multiplied by 2 (so that it is same as Eq. (2) in Ref. [21]).

For the evolution of ρ_ϕ and T , the equations are almost same as those found in Ref. [22]. We just need modifications due to our use of scale factor a as a time variable and discrimination of ν_μ from ν_τ . For ρ_ϕ , it is given by

$$\frac{d\rho_\phi}{da} = -\frac{\Gamma}{aH}\rho_\phi - \frac{3}{a}\rho_\phi. \quad (19)$$

The equation of the total energy-momentum conservation is

$$\frac{d\rho_{\text{tot}}}{da} = -\frac{3}{a}(\rho_{\text{tot}} + P_{\text{tot}}), \quad (20)$$

where the total energy density and the total pressure are given by

$$\begin{aligned} \rho_{\text{tot}} &\equiv \rho_\phi + \rho_\gamma + \rho_{e^\pm} + \rho_{\nu_e} + \rho_{\nu'_\mu} + \rho_{\nu'_\tau} \\ &= \rho_\phi + \frac{\pi^2 T^4}{15} + \frac{2}{\pi^2} \int_0^\infty dp p^2 \frac{E_e}{\exp(E_e/T) + 1} \\ &\quad + \frac{1}{\pi^2 a^4} \int_0^\infty dy y^3 (f_{\nu_e} + f_{\nu'_\mu} + f_{\nu'_\tau}), \end{aligned} \quad (21)$$

$$\begin{aligned} P_{\text{tot}} &\equiv P_\gamma + P_{e^\pm} + P_{\nu_e} + P_{\nu'_\mu} + P_{\nu'_\tau}, \\ &= \frac{\pi^2 T^4}{45} + \frac{2}{3\pi^2} \int_0^\infty dp \frac{p^4}{E_e (\exp(E_e/T) + 1)} \\ &\quad + \frac{1}{3\pi^2 a^4} \int_0^\infty dy y^3 (f_{\nu_e} + f_{\nu'_\mu} + f_{\nu'_\tau}) \end{aligned} \quad (22)$$

with the electron energy $E_e \equiv \sqrt{m_e^2 + p^2}$. The evolution equation for T is derived from Eq. (20):

$$\begin{aligned} \frac{dT}{da} &= -\left(\frac{\partial \rho_\gamma}{\partial T} + \frac{\partial \rho_{e^\pm}}{\partial T}\right)^{-1} \left\{ \frac{4}{a}\rho_\gamma + \frac{3}{a}(\rho_{e^\pm} + P_{e^\pm}) - \frac{\Gamma}{aH}\rho_\phi \right. \\ &\quad \left. + \frac{1}{\pi^2 a^4} \int_0^\infty dy y^3 \left(\frac{df_{\nu_e}}{da} + \frac{df_{\nu'_\mu}}{da} + \frac{df_{\nu'_\tau}}{da} \right) \right\} \end{aligned} \quad (23)$$

Finally, the expansion rate is

$$H \equiv \frac{1}{a} \frac{da}{dt} = \frac{\sqrt{\rho_{\text{tot}}}}{\sqrt{3}M_{\text{Pl}}}. \quad (24)$$

To integrate the differential equations, since the equations for $f_\nu(y)$ are stiff, we used semi-implicit extrapolation method [35]. Using the Ref. [35]'s implementation which incorporates adaptive stepsize control routine, we were able to evolve the neutrino density matrices very efficiently. We followed the evolution well after the electron-positron annihilation ends and $f_\nu(y)$'s become constant.

As for the initial condition, we have to make the inflaton energy density dominate the universe at first. As long as ρ_ϕ is much larger than radiation energy density ($\sim T^4$), evolution afterward does not depend on their precise values. In this paper, we adopt rather realistic relation between ρ_ϕ and ρ_{rad} ,

$$\rho_{\text{rad}} = \frac{2\sqrt{3}}{5}\Gamma M_{\text{Pl}}\rho_\phi^{1/2}, \quad (25)$$

which derived from the analytic solutions during the epoch of coherent oscillations [34].

III. RESULTS AND COSMOLOGICAL IMPLICATIONS

In this section, we present the results of our numerical calculation for neutrino thermalization and consider its implications for cosmology. We evolve the neutrino density matrices with various values of the reheating temperature T_R and investigate how the neutrino distribution functions, neutrino energy densities and big bang nucleosynthesis depend on T_R . Along with the neutrino thermalization with oscillations, we show the results without oscillations which have been studied in Refs [21, 22, 23] and elucidate the neutrino oscillation effects on a low reheating temperature scenario. Our results when the oscillations are omitted turn out to be consistent with those of previous papers. We find that the inclusion of the oscillations most characteristically alters the ^4He synthesis and its abundance varies with respect to T_R quite differently from the no oscillation case .

A. Neutrino distribution functions

We show the final neutrino distribution functions in Figs. 1 (a)-(d) for the cases of $T_R = 15$ MeV and 2.5 MeV respectively with and without the oscillations. We see from Figs. 1 (a) and (b) that when the reheating temperature is sufficiently high, all the neutrino species are thermalized regardless of the oscillations.

However, for the case of lower reheating temperature, the oscillations significantly matter as seen from comparing Figs. 1 (c) and (d) : f_{ν_e} and f_{ν_μ} are almost equalized by the solar mixing. When the oscillations are neglected, f_{ν_e} becomes much larger than f_{ν_μ} as shown in Fig. 1 (c) because ν_e is produced by the charged current interaction in addition to the neutral current interaction but ν_μ and ν_τ are produced only by the latter [21, 22]. When

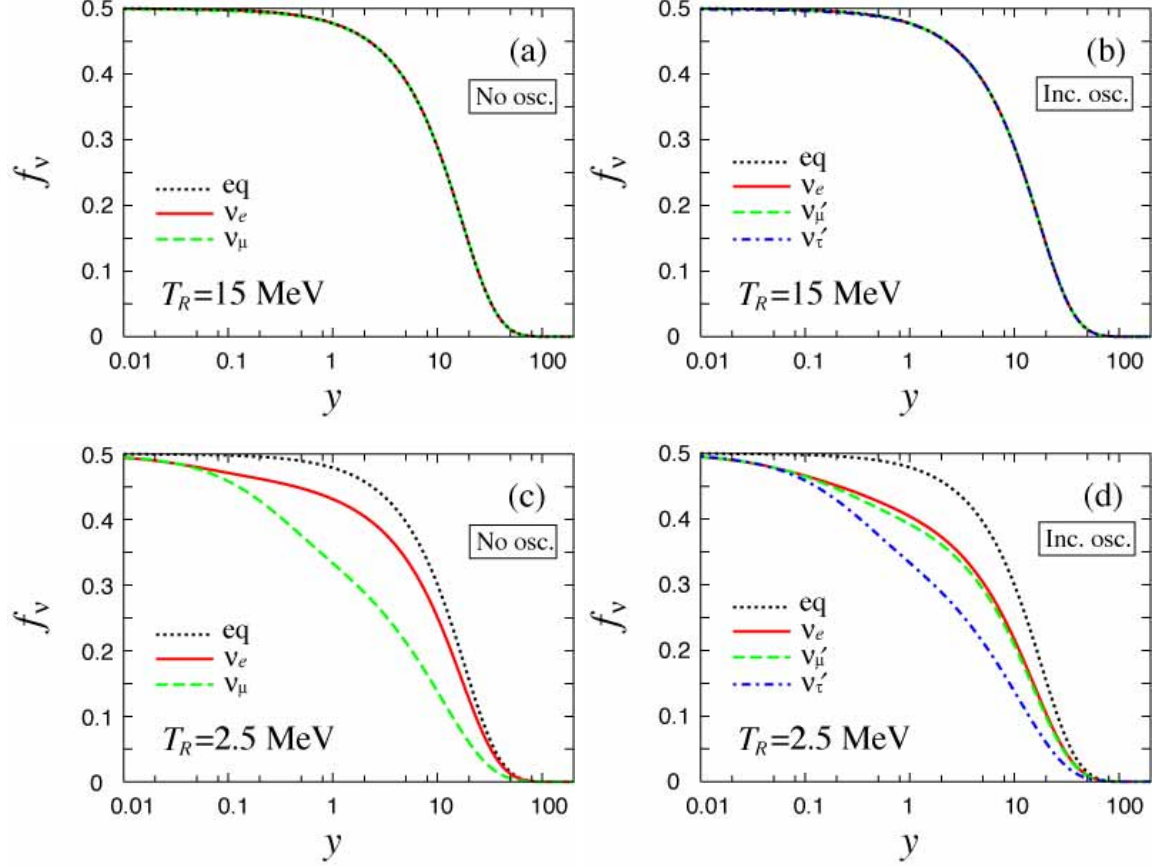


FIG. 1: The final distribution functions of neutrinos. (a) and (c) are cases for no oscillations (ν_e is displayed by solid lines and ν_μ by dashed lines) and (b) and (d) incorporate the oscillations (ν_e is displayed by solid lines, ν'_μ by dashed lines and ν'_τ by dot-dashed lines). The equilibrium distributions are drawn by dotted lines in order to show how much they are thermalized. For $T_R = 15$ MeV, in (a) and (b), whether the oscillations are present or not, all the lines overlap and this means every neutrino species is fully thermalized for high reheating temperature. For $T_R = 2.5$ MeV, in (c) and (d), distributions are away from equilibrium form. When the oscillations are taken into account, distributions of ν_e and ν'_μ get close as seen in (d).

there are the flavor mixings, ν_e and ν'_μ can convert into each other. ν'_μ is now produced also by the oscillations from ν_e which exists more than ν'_μ so $f_{\nu'_\mu}$ increases compared to no oscillation case. On the contrary, f_{ν_e} becomes smaller when the oscillations are included naturally because ν_e oscillates into ν'_μ . However, this deficit is to some extent filled by the ν_e production from the thermal plasma so the neutrinos are produced more in total under the existence of the oscillations. This is seen in Fig. 2 which shows clearly that $f_{\nu_e} + f_{\nu'_\mu}$

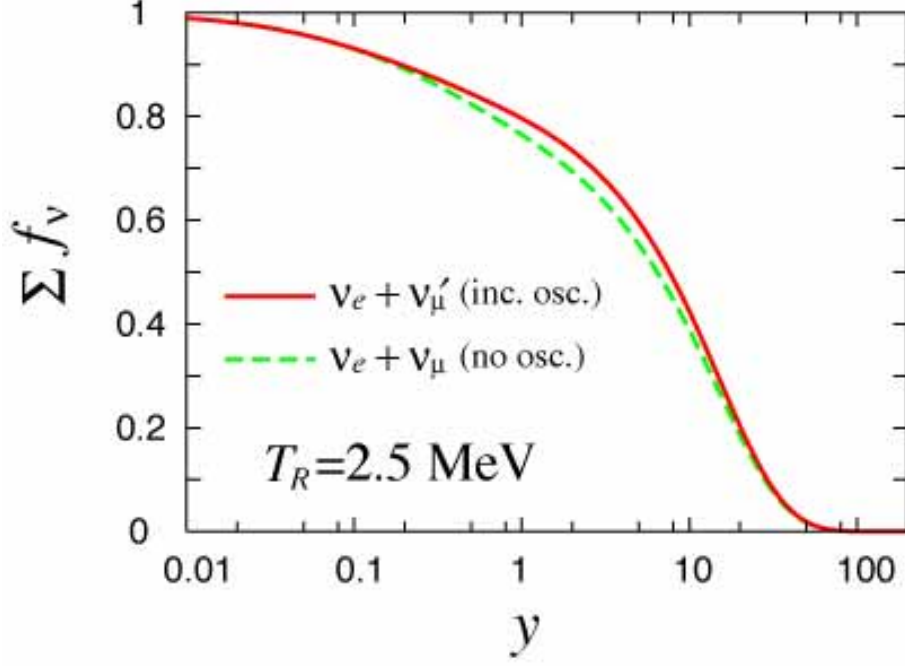


FIG. 2: We draw the sums of the distribution functions, $f_{\nu_e} + f_{\nu_\mu}$ (no oscillation) and $f_{\nu_e} + f_{\nu'_\mu}$ (including oscillation) with the dashed line and the solid line respectively. The latter is larger showing that the oscillations make the thermalization more efficient in total.

(including oscillation) $> f_{\nu_e} + f_{\nu_\mu}$ (no oscillation).

B. Effective number of neutrinos

Let us discuss our results of the neutrino thermalization in terms of neutrino energy density. This is often expressed using the effective number of neutrinos N_ν . This number is observationally relevant to the CMB power spectrum and large scale structure. It is given by

$$N_\nu \equiv \frac{\sum \rho_\nu}{\rho_{\nu,\text{std}}}, \quad (26)$$

where the summation is taken for $\nu = \nu_e, \nu_\mu$, and ν_τ when the oscillations are not included and $\nu = \nu_e, \nu'_\mu$, and ν'_τ when we consider the oscillations. We define $\rho_{\nu,\text{std}}$ using the photon temperature T as

$$\rho_{\nu,\text{std}} = \frac{7\pi^2}{120} \left\{ \left(\frac{4}{11} \right)^{1/3} T \right\}^4, \quad (27)$$

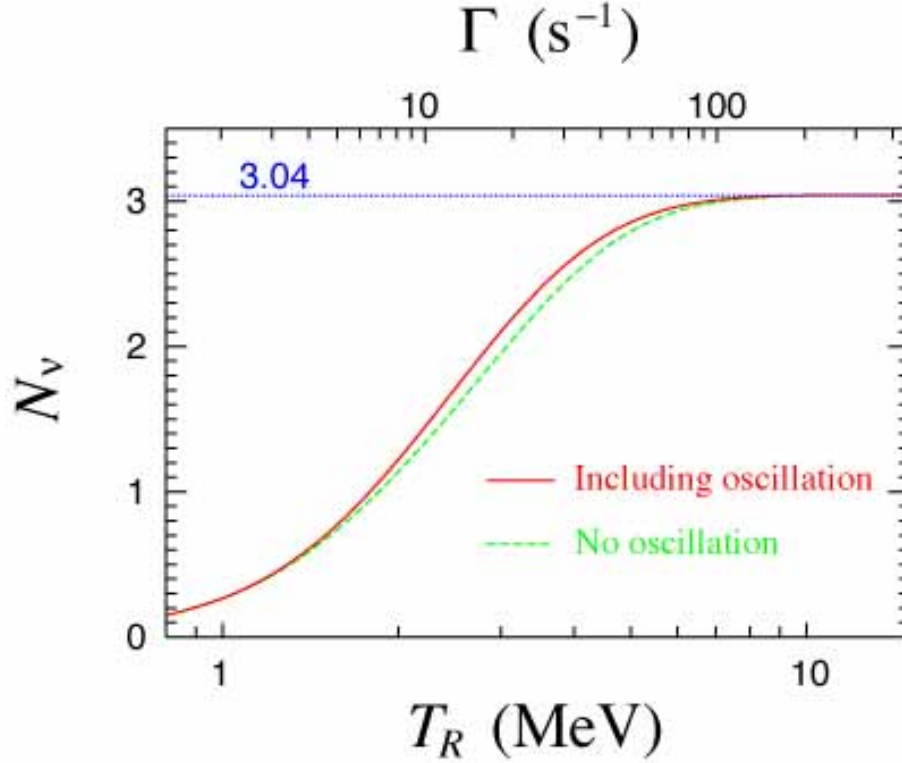


FIG. 3: The effective neutrino number N_ν as a function of the reheating temperature T_R (shown on the bottom abscissa) or the decay width Γ (shown on the top abscissa). The cases with and without the oscillations are drawn respectively by the solid and dashed lines. The horizontal line denotes $N_\nu = 3.04$ with which N_ν for high T_R should coincide (see the text).

which corresponds to the neutrino energy density assuming that neutrinos are completely decoupled from the rest of the thermal plasma before the electron-positron annihilation takes place. If this assumption is exact, N_ν would be 3. It is actually a very good assumption but detailed calculations on the entropy transfer from electrons to neutrinos have shown that ρ_ν 's are slightly larger than $\rho_{\nu,\text{std}}$ and $N_\nu = 3.04$ [18, 19, 20, 28].

We calculate ρ_ν by integrating the final neutrino distribution functions such as presented in Fig. 1, and derive N_ν as a function of the reheating temperature T_R . The result is shown in Fig. 3. For $T_R \gtrsim 10$ MeV, N_ν asymptotes the value 3.04 which indicates thermalized neutrino distributions. This is regardless of the neutrino oscillations and consistent with Fig. 1 (a) and (b) discussed in section III A. For the smaller values of T_R , the inclusion of the oscillations make N_ν larger as expected from Fig. 2. This effect is most conspicuous for

$T_R = 2 \sim 5$ MeV and changes N_ν up to ~ 0.2 .

Fig. 3 enables us to constrain T_R by using the limits on the effective number of neutrino species from cosmological observations such as CMB and galaxy surveys. Recent papers, Refs. [36, 37, 38, 39], derive the lower limit to be $0.9 \sim 1.9$ (these are the limits obtained without resorting to BBN. Some of them have also reported more stringent limits obtained using data combined with observed Y_p . However, since they assume Fermi-Dirac distribution for neutrinos and only modify the Friedmann equation when they calculate Y_p , we cannot use those limits. This point is discussed in section III C in detail). If $N_\nu > 0.9$ is adopted, the bound on the reheating temperature is $T_R > 1.69$ MeV with the oscillations and $T_R > 1.74$ MeV for no oscillation case.

C. Light element abundances

We now investigate how the big bang nucleosynthesis is affected by the non-thermal neutrino distributions and/or the neutrino oscillations. We calculate the light element (D, ^4He and ^7Li) abundances as functions of T_R , again with and without the neutrino oscillations. The cosmological effects of incomplete neutrino thermalization is most strikingly seen in ^4He abundance since electron-type neutrinos play a special role in determining the rate of neutron-proton conversion during BBN. This has been already known from the previous papers Refs. [21, 22] in which the oscillations are neglected, but we find that the neutrino oscillations prominently matter in regard to the T_R -dependence of ^4He abundance.

We show how Y_p varies with respect to T_R in Fig. 4. This is calculated by plugging the solutions of the evolution equations derived in section II into the Kawano BBN code [40] (with updated reaction rates compiled by Angulo et al. [41]). Required modifications are the temperature dependence of the neutron-proton conversion rates, $\Gamma_{n \rightarrow p}$ and $\Gamma_{p \rightarrow n}$, and the evolution equation for the photon temperature. The calculation of $\Gamma_{n \leftrightarrow p}$ (see e.g. Ref. [42]) involves the integration of the electron neutrino distribution function f_{ν_e} which does not necessarily take the Fermi distribution form in our case. For the photon temperature evolution, the contributions from ϕ and neutrinos are supplemented in the same way as Eq. (23).

There are two effects caused by incomplete thermalization of neutrinos competing to make up the dependence of Y_p on T_R as shown in Fig. 4: slowing down of the expansion rate

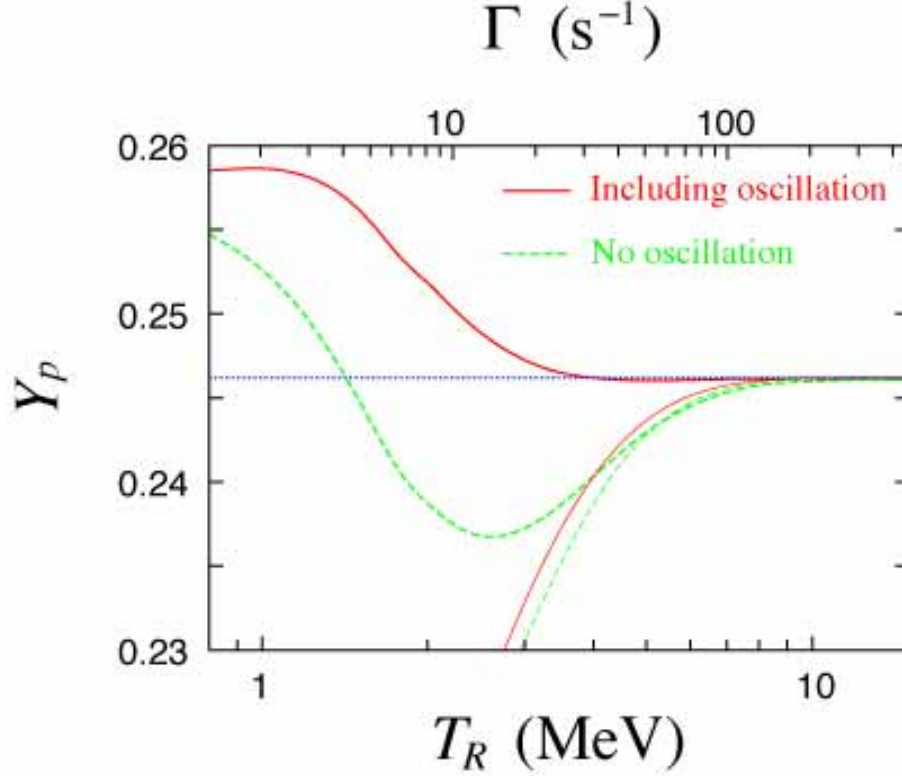


FIG. 4: The ${}^4\text{He}$ abundance (mass fraction) Y_p as a function of the reheating temperature T_R (shown on the bottom abscissa) or the decay width Γ (shown on the top abscissa). The cases with and without the oscillations are drawn respectively by the solid and dashed curves. Thinner curves are calculated with fermi distributed neutrinos with N_ν of Fig. 3 (namely, only the change in the expansion rate due to the incomplete thermalization is taken into account). The horizontal line represents “standard ” Y_p calculated by BBN with neutrinos obeying the fermi distribution and $N_\nu = 3.04$. The baryon-to-photon ratio is fixed at $\eta = 5 \times 10^{-10}$.

and decreasing in $\Gamma_{n \leftrightarrow p}$. The former is just a result of the decrease in the neutrino energy density (of all species). The latter is due to the deficit in f_{ν_e} . They compete in a sense that they work in opposite way to determine the epoch of neutron-to-proton ratio freeze-out: the former makes it later and the latter makes it earlier. Then, the competition fixes the n-p ratio at the beginning of nucleosynthesis and eventually determine Y_p . Roughly speaking, for larger T_R , the former dominates to decrease Y_p but, for smaller T_R , the latter dominates and increase Y_p . This is clearly seen in the case without the oscillations but not for the case including the oscillations because the incompleteness in the ν_e thermalization is made

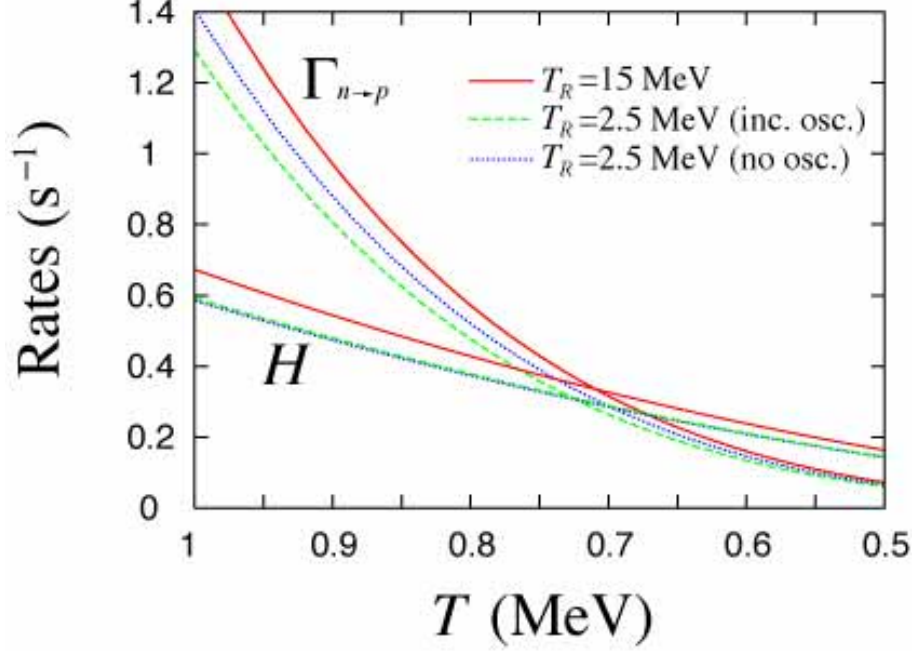


FIG. 5: The weak interaction rate $\Gamma_{n\rightarrow p}$ and the expansion rate H as functions of temperature, where $\Gamma_{n\rightarrow p}$ and H first become equal. We plot for $T_R = 2.5$ MeV with and without the oscillations. For $T_R = 15$ MeV, the oscillations do not make any difference.

severer by the mixing (see the panels (c) and (d) in Fig. 1) and this effect dominates already at high T_R .

Before going forward, it may be worthwhile to look slightly more into the explanation of the T_R -dependence of Y_p . First, let us forget about modifying $\Gamma_{n\leftrightarrow p}$ or temperature evolution and just calculate ${}^4\text{He}$ abundance using thermally distributed neutrinos with N_ν 's indicated in Fig. 3 for each value of T_R . This corresponds to including the effect of slowing down the expansion rate due to the incomplete thermalization but neglecting the electron neutrino deficiency. Accordingly, lowering T_R only acts to delay the n-p ratio freeze-out and decrease Y_p (shown by the thinner curves in Fig. 4). In actual low-reheating temperature scenario, a lack of ν_e reduces $\Gamma_{n\leftrightarrow p}$. This counterbalances the effect of slowing-down expansion and boosts Y_p in total at lower T_R . To see this is really the case, we plot $\Gamma_{n\rightarrow p}$ for some values of T_R in Fig. 5. We see that $\Gamma_{n\rightarrow p}$ is smaller for lower T_R which is attributed to less thermalized ν_e . It is also instructive to calculate the neutron-to-proton ratio freeze-out temperature T_{np} , which we define by $\Gamma_{n\rightarrow p}(T_{\text{np}}) = H(T_{\text{np}})$, to confirm where the competition settles. This

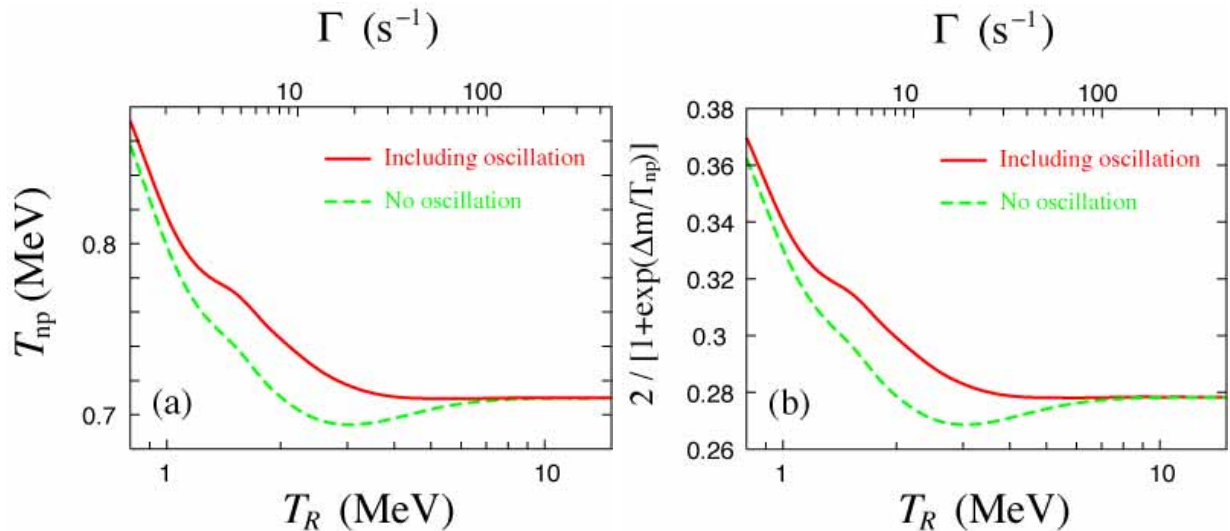


FIG. 6: (a) T_{np} , freeze-out temperature of the neutron-to-proton ratio, and (b) $2/[1 + \exp(\Delta m/T_{np})]$, as functions of T_R .

is shown in Fig. 6 (a) and we see that at low T_R , the decrease in $\Gamma_{n \rightarrow p}$ wins to make T_{np} higher (in the case with the oscillations, this seems to win for every T_R and T_{np} rises monotonically as T_R decreases). We note that the figure well reproduces the profile found in Fig. 4. This resemblance becomes more meaningful by plotting instead the quantity $2/[1 + (n_p/n_n)_f] = 2/[1 + \exp(\Delta m/T_{np})]$, the usual estimation of ^4He abundance from the neutron-to-proton ratio at the freeze-out value, which is shown in Fig. 6 (b). Although the figure is not exactly same as Fig. 4 because free decays of neutrons are not considered, we see that the Y_p 's dependence on T_R is sufficiently understood from this estimation. When the neutron free decay is properly taken into account, the estimation for Y_p decreases from the values indicated in Fig. 6 (b). For lower T_R , since the time between T_{np} and the start of the nucleosynthesis ($T \approx 0.07$ MeV) is longer (this in turn is explained by the smaller expansion rate due to less neutrino energy densities), this decrease should be larger. Therefore, on including the neutron free decay, Fig. 6 (b) would be tilted toward left (smaller T_R) side and should look more like Fig. 4. In particular, the minimum found for the case without the oscillations should be located at lower T_R when the free decay is included.

We have so far discussed the ^4He synthesis features common to the low- T_R universe with and without the neutrino oscillations, but we would rather like to emphasize that there is a striking difference between them. This is most clearly visible in Fig. 4: when we include

the oscillations, Y_p does not decrease if we lower T_R . This is somewhat surprising because, at the same time, N_ν becomes smaller (see Fig. 3). This means that, in the case with the oscillations, the effect of slowing down cosmic expansion (as represented by decreasing N_ν) is completely overcome by the decrease in $\Gamma_{n\leftrightarrow p}$ for all T_R . The reason why this happens is that since the oscillations convert electron neutrinos into muon neutrinos, the deficiency in electron neutrinos is made severer (see Fig. 2). Moreover, why this matters for ${}^4\text{He}$ synthesis is that it is exclusively sensitive to the ν_e distribution function which determines $\Gamma_{n\leftrightarrow p}$. On the other hand, the structure formation is affected only by the energy density so it does not distinguish neutrino flavors. Since only their sum matters, the oscillations scarcely make difference (see Fig. 3). Therefore, BBN, especially when the neutrino oscillations are taken into account, turns out to be unique probe of low reheating temperature scenario. Next, we proceed to compare the predictions of the scenario with the observed abundances.

On comparing the predictions of low reheating temperature scenario with the observed abundances, we need to vary the baryon-to-photon ratio, η , which is the input parameter for the standard BBN calculation, in addition to T_R . In Fig. 7 we show contour plots for abundances of light elements, D, ${}^4\text{He}$ and ${}^7\text{Li}$, against η and T_R . Since contours tend to be parallel to each other, we see that how abundances vary with respect to T_R has little dependence on η . In particular, for ${}^4\text{He}$, features found in Fig. 4 seem to appear at every η . We notice, in Fig. 7 (c) and (d), that the oscillations almost do not make difference for D and ${}^7\text{Li}$ abundances. In the figure, we also indicate observed values taken from Ref. [43] for ${}^4\text{He}$, from Ref. [44] for D, and from Ref. [45] for ${}^7\text{Li}$:

$$Y_p = 0.238 \pm 0.002 \pm 0.005, \quad (28)$$

$$\text{D}/\text{H} = 2.78^{+0.44}_{-0.38} \times 10^{-5}, \quad (29)$$

$${}^7\text{Li}/\text{H} = 1.23^{+0.68}_{-0.32} \times 10^{-10} \quad (95\%) \quad (30)$$

In Eq. (28), the first uncertainty is statistical and the second one is systematic. Their root-mean-square, $[(\text{stat.})^2 + (\text{syst.})^2]^{1/2}$, is adopted as overall 1σ error. In this paper, we do not consider the ${}^7\text{Li}$ data since its systematic error is under debate at present, but show it just for reference ⁵.

⁵ It is known that the baryon density derived from Eq. (28) is somewhat lower than one from Eq. (29). It was widely believed that $N_\nu < 3$ decreases Y_p and ameliorates this tension (see e.g., Ref. [46]). However

We immediately realize from Fig. 7 (a), (b), (c) that inclusion of the oscillations leaves smaller room for the low reheating temperature scenario. In other words, the parameter region allowed from D and ^4He measurements is smaller for the case with the neutrino oscillation. We can see it more clearly by χ^2 -analysis whose results are shown in Fig. 8. The lower bound on T_R at 95% confidence level in the η - T_R plane is 1 MeV for the case of no oscillations but tightened to be 2 MeV for the case incorporating the oscillations⁶.

IV. CONCLUSION

In this paper we have investigated the MeV-scale reheating scenario wherein the thermalization of neutrinos could be insufficient. We have paid particular attention to the oscillation effects on the thermalization processes of neutrinos, and solved numerically the momentum dependent Boltzmann equations for neutrino density matrix, fully taking account of neutrino oscillations. In contrast to the widespread picture, we have found that ^4He abundance does increase while the effective neutrino number N_ν decreases. The reason is simple; the neutrino oscillations reduce the number density of ν_e , due to which the neutron-proton transformation decouples earlier. This effect cancels and even exceeds that of the decrease in the expansion rate; only the latter effect has been usually taken into account when discussing the effect of N_ν on the light-element abundances. Therefore we would like to stress that it is indispensable to take into consideration the oscillation effects, to set a lower bound on the reheating temperature by using the BBN. As a reference value, we quote our results; $T_{RH} \gtrsim 2 \text{ MeV}$ or equivalently $N_\nu \gtrsim 1.2$ obtained by using the observational data on the ^4He and D abundances.

What are then the distinct predictions of the MeV-scale reheating? Clearly, they are: both larger Y_p and smaller N_ν compared to their standard values; if both the observed Y_p and N_ν suggest the same T_R by the relations shown in Figs. 3 and 4, they would serve as

we now know this is not feasible simply by lowering the reheating temperature if we properly take into account neutrino oscillations.

⁶ Recently, analysis of the ^4He abundance by Ref. [47] suggests $Y_p = 0.249 \pm 0.009$ [48]. This is higher than the value of Eq. (28) mainly due to the different treatments of stellar absorption. Although, at present, such large uncertainty does not allow us to derive any meaningful lower bound on T_R . However, higher Y_p is interesting for MeV-scale reheating scenario. Should future research yield $Y_p > 0.25$, $T_R \sim O(\text{MeV})$ would be favored.

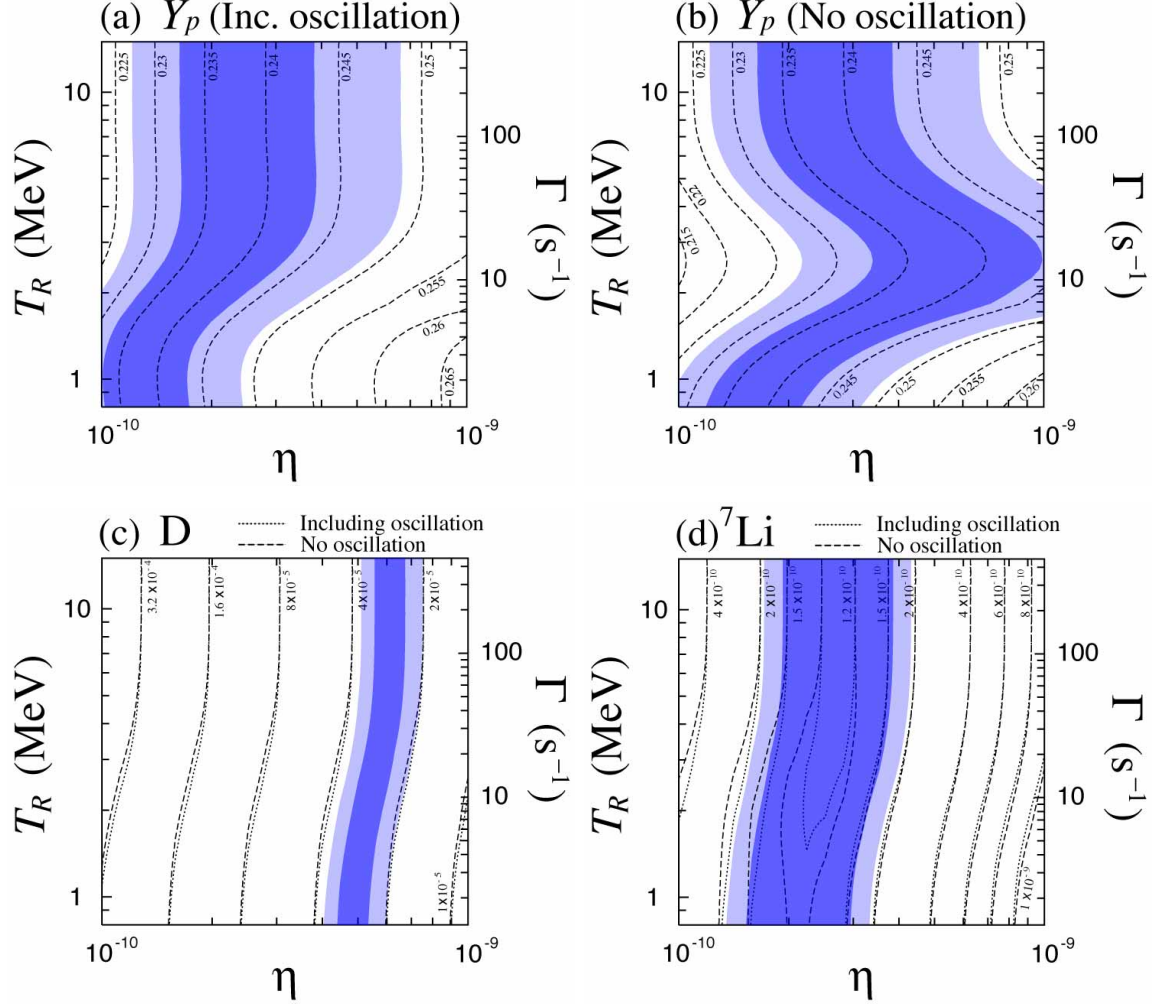


FIG. 7: Contour plots for the light element abundances. ${}^4\text{He}$ mass fraction is plotted in (a) with the oscillations and in (b) without. D and ${}^7\text{Li}$ are plotted respectively in (c) and (d) where dotted lines express the case with the oscillations and dashed lines express the case without. Shaded areas represent uncertainties in the observed abundances expressed in eqs. (28) \sim (30) (for D and ${}^7\text{Li}$, they are drawn against the contours considering the oscillations). Darker areas are for 1σ and lighter for 2σ .

decisive evidence for the MeV-scale reheating.

At last, let us comment on the validity and possible extension of the present work. As explained in section II, we have neglected the self-interactions of neutrinos. Such simplification is considered to be valid since the number of neutrinos is less than the equilibrium value. However, the self-interactions have a potential effect on the number density of ν_e

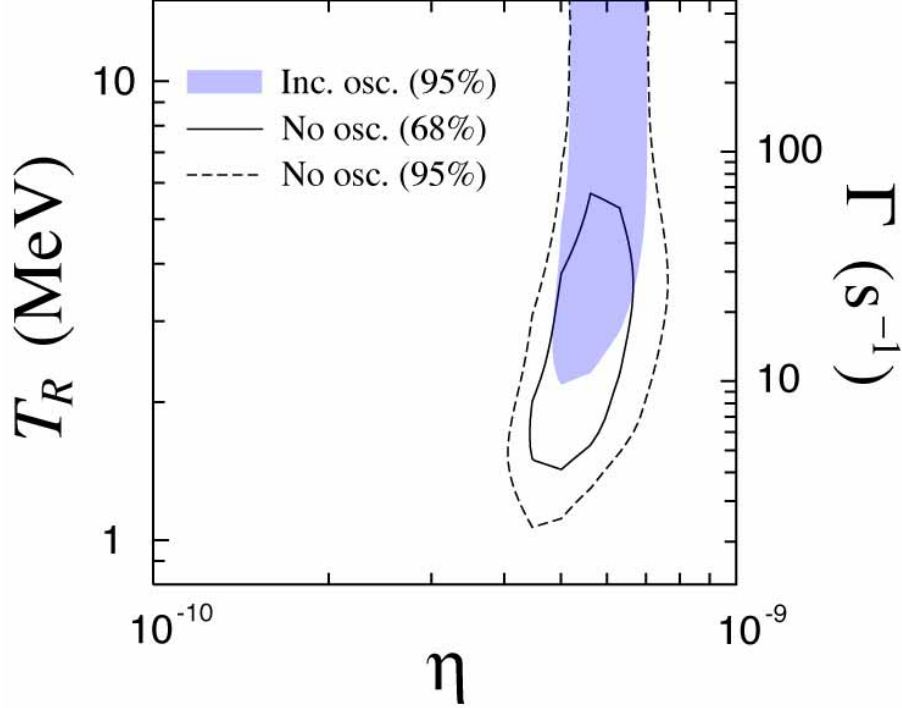


FIG. 8: χ^2 contour plot using data of D and ^4He . For no oscillation case, the allowed regions at 68% and 95% confidence levels are drawn with solid and dashed lines. For the case with oscillations, the 68% allowed region does not appear and only the 95% region is indicated by the shaded area.

through e.g., $\nu_e \bar{\nu}_e \leftrightarrow \nu_{\mu(\tau)} \bar{\nu}_{\mu(\tau)}$. Furthermore, nonzero θ_{13} can have a similar effect; in this case it is necessary to perform three generation analysis. Nevertheless we believe that our main conclusion does not change, since these extensions, too, are expected to decrease the number density of ν_e , further increasing the ^4He abundance. Of course the quantitative improvement should be necessary and the full analysis on these points will be presented elsewhere [49].

Acknowledgments.— F.T. would like to thank the Japan Society for Promotion of Science for financial support.

[1] D. N. Spergel *et al.* [WMAP Collaboration], *Astrophys. J. Suppl.* **148**, 175 (2003).

[2] M. Kawasaki, K. Kohri and T. Moroi, arXiv:astro-ph/0402490;

M. Kawasaki, K. Kohri and T. Moroi, *Phys. Rev. D* **71**, 083502 (2005).

- [3] G. D. Coughlan, W. Fischler, E. W. Kolb, S. Raby and G. G. Ross, Phys. Lett. B **131**, 59 (1983).
- [4] T. Banks, D. B. Kaplan and A. E. Nelson, Phys. Rev. D **49**, 779 (1994).
- [5] B. de Carlos, J. A. Casas, F. Quevedo and E. Roulet, Phys. Lett. B **318**, 447 (1993).
- [6] M. Kawasaki, K. Kohri and T. Moroi, Phys. Rev. D **63**, 103502 (2001).
- [7] K. Jedamzik, Phys. Rev. Lett. **84**, 3248 (2000).
- [8] R. H. Cyburt, J. R. Ellis, B. D. Fields and K. A. Olive, Phys. Rev. D **67**, 103521 (2003).
- [9] D. H. Lyth and E. D. Stewart, Phys. Rev. Lett. **75**, 201 (1995);
D. H. Lyth and E. D. Stewart, Phys. Rev. D **53**, 1784 (1996).
- [10] M. Kawasaki and F. Takahashi, arXiv:hep-ph/0410158.
- [11] K. Enqvist and M. S. Sloth, Nucl. Phys. B **626** (2002) 395;
D. H. Lyth and D. Wands, Phys. Lett. B **524** (2002) 5;
T. Moroi and T. Takahashi, Phys. Lett. B **522** (2001) 215 [Erratum-ibid. B **539** (2002) 303];
T. Moroi and T. Takahashi, Phys. Rev. D **66**, 063501 (2002).
- [12] I. Affleck and M. Dine, Nucl. Phys. B **249**, 361 (1985);
M. Dine, L. Randall and S. Thomas, Nucl. Phys. B **458**, 291 (1996).
- [13] S. R. Coleman, Nucl. Phys. B **262**, 263 (1985) [Erratum-ibid. B **269**, 744 (1986)];
A. Kusenko and M. E. Shaposhnikov, Phys. Lett. B **418**, 46 (1998);
K. Enqvist and J. McDonald, Nucl. Phys. B **538**, 321 (1999);
S. Kasuya and M. Kawasaki, Phys. Rev. D **61**, 041301 (2000);
S. Kasuya and M. Kawasaki, Phys. Rev. D **62**, 023512 (2000).
- [14] M. Kawasaki, F. Takahashi and M. Yamaguchi, Phys. Rev. D **66**, 043516 (2002).
- [15] S. Kasuya, M. Kawasaki and F. Takahashi, Phys. Lett. B **578**, 259 (2004).
- [16] K. Hamaguchi, M. Kawasaki, T. Moroi and F. Takahashi, Phys. Rev. D **69**, 063504 (2004).
- [17] K. Ichikawa, M. Kawasaki and F. Takahashi, Phys. Lett. B **597**, 1 (2004).
- [18] S. Hannestad and J. Madsen, Phys. Rev. D **52**, 1764 (1995).
- [19] A. D. Dolgov, S. H. Hansen and D. V. Semikoz, Nucl. Phys. B **503**, 426 (1997).
- [20] A. D. Dolgov, S. H. Hansen and D. V. Semikoz, Nucl. Phys. B **543**, 269 (1999).
- [21] M. Kawasaki, K. Kohri and N. Sugiyama, Phys. Rev. Lett. **82**, 4168 (1999).
- [22] M. Kawasaki, K. Kohri and N. Sugiyama, Phys. Rev. D **62**, 023506 (2000).
- [23] S. Hannestad, Phys. Rev. D **70**, 043506 (2004).

- [24] Y. Fukuda *et al.* [Super-Kamiokande Collaboration], Phys. Rev. Lett. **81**, 1562 (1998);
Y. Ashie *et al.* [Super-Kamiokande Collaboration], arXiv:hep-ex/0501064.
- [25] B. T. Cleveland *et al.*, Astrophys. J. **496**, 505 (1998);
J. N. Abdurashitov *et al.* [SAGE Collaboration], Nucl. Phys. Proc. Suppl. **118**, 39 (2003);
T. A. Kirsten [GNO Collaboration], Nucl. Phys. Proc. Suppl. **118**, 33 (2003);
S. Fukuda *et al.* [Super-Kamiokande Collaboration], Phys. Rev. Lett. **86**, 5656 (2001);
B. Aharmim *et al.* [SNO Collaboration], arXiv:nucl-ex/0502021;
T. Araki *et al.* [KamLAND Collaboration], Phys. Rev. Lett. **94**, 081801 (2005).
- [26] G. Sigl and G. Raffelt, Nucl. Phys. B **406**, 423 (1993).
- [27] S. Esposito, G. Miele, S. Pastor, M. Peloso and O. Pisanti, Nucl. Phys. B **590**, 539 (2000).
- [28] G. Mangano, G. Miele, S. Pastor and M. Peloso, Phys. Lett. B **534**, 8 (2002).
- [29] A. D. Dolgov, S. H. Hansen, S. Pastor, S. T. Petcov, G. G. Raffelt and D. V. Semikoz, Nucl. Phys. B **632**, 363 (2002).
- [30] K. Ichikawa and M. Kawasaki, Phys. Lett. B **570**, 154 (2003).
- [31] K. N. Abazajian, J. F. Beacom and N. F. Bell, Phys. Rev. D **66**, 013008 (2002).
- [32] A. D. Dolgov and F. Takahashi, Nucl. Phys. B **688**, 189 (2004).
- [33] G. L. Fogli, E. Lisi, A. Marrone, D. Montanino, A. Palazzo and A. M. Rotunno, eConf C030626 (2003) THAT05 [arXiv:hep-ph/0310012].
- [34] E. W. Kolb and M. S. Turner, *The Early Universe* (Addison Wesley, Reading, MA, 1990).
- [35] W. H. Press, B. P. Flannery, S. A. Teukolsky and W. T. Vetterling, *Numerical Recipes* (Cambridge University Press, New York, 1986).
- [36] P. Crotty, J. Lesgourgues and S. Pastor, Phys. Rev. D **67**, 123005 (2003).
- [37] E. Pierpaoli, Mon. Not. Roy. Astron. Soc. **342**, L63 (2003).
- [38] S. Hannestad, JCAP **0305**, 004 (2003).
- [39] V. Barger, J. P. Kneller, H. S. Lee, D. Marfatia and G. Steigman, Phys. Lett. B **566**, 8 (2003).
- [40] L. H. Kawano, FERMILAB-Pub-92/04-A (1992).
- [41] C. Angulo *et al.*, Nucl. Phys. A. **656**, 3 (1999).
- [42] S. Weinberg, *Gravitation and Cosmology*, (John Wiley & Sons, New York, 1972).
- [43] B. D. Fields and K. A. Olive, Astrophys. J. **506**, 177 (1998).
- [44] D. Kirkman, D. Tytler, N. Suzuki, J. M. O'Meara and D. Lubin, Astrophys. J., Suppl. Ser. **149**, 1 (2003).

- [45] S. G. Ryan, T. C. Beers, K. A. Olive, B. D. Fields, and J. E. Norris, *Astrophys. J. Lett.*, **530**, L57 (2000).
- [46] K. Ichikawa and M. Kawasaki, *Phys. Rev. D* **69**, 123506 (2004).
- [47] K. A. Olive and E. D. Skillman, *Astrophys. J.* **617**, 29 (2004).
- [48] R. H. Cyburt, B. D. Fields, K. A. Olive and E. Skillman, *Astropart. Phys.* **23**, 313 (2005).
- [49] K. Ichikawa, M. Kawasaki and F. Takahashi, in preparation.